Comparison of amyloid PET measured in Centiloid units with neuropathological findings in Alzheimer's Disease

Sanka Amadoru (sanka.amadoru@austin.org.au)
Austin Health https://orcid.org/0000-0002-0522-6143
Vincent Doré
CSIRO
Catriona A McLean
The Florey Institute of Neuroscience and Mental Health
Fairlie Hinton
The Florey Institute of Neuroscience and Mental Health
Claire E Shepherd
University of New South Wales
Glenda M Halliday
University of New South Wales
Cristian E Leyton
University of Sydney
Paul A Yates
Austin Health
John R Hodges
University of Sydney
Colin L Masters
The Florey Institute of Neuroscience and Mental Health
Victor L Villemagne
Austin Health
Christopher C Rowe
Austin Health

Research

Keywords: Amyloid imaging, Alzheimer's disease, Centiloids, positron emission tomography, neuropathology.

Posted Date: November 9th, 2019

DOI: https://doi.org/10.21203/rs.2.17082/v1

Version of Record: A version of this preprint was published at Alzheimer's Research and Therapy on March 4th, 2020. See the published version at https://doi.org/10.1186/s13195-020-00587-5.

Abstract

Background: We aimed to determine the Centiloid unit (CL) thresholds for sparse and moderate density neuritic plaques. Methods: Amyloid PET results in CL for 49 subjects were compared with post-mortem neuritic plaque density, visual read, and final clinicopathological diagnosis. A Youden Index was used to determine the optimal CL thresholds from receiver operator characteristic (ROC) curves. Results: A threshold of 20.1 CL yielded highest accuracy in detecting moderate or frequent plaque density (ROC AUC 0.97). A threshold of 9.5 CL was optimal for detecting sparse, moderate or frequent plaques (ROC AUC 0.96). Those cases with a final clinicopathological diagnosis of Alzheimer's disease yielded a median CL result of 87.7 (IQR ±42.2) with 94% > 45 CL. Positive visual read agreed highly with results >26 CL. Conclusions: In this cohort, values <9.5 CL accurately reflected the absence of any neuritic plaques, and >20.1 CL indicated the presence of at least moderate plaque density. Clinicopathological diagnosis of AD was rare with CL <45.

Background

Current standard-of-truth (SoT) diagnosis of Alzheimer's disease (AD) partly depends on neuropathological demonstration of brain amyloid-beta (Aβ) plaques and tau [1]. However, the invasive nature of brain biopsy requires antemortem diagnosis to be made using biomarkers. Recently, research criteria for AD have emphasized the importance of amyloid and tau positron emission tomography (PET) imaging biomarkers [2, 3].

^{11}C-Pittsburgh Compound B (^{11}C-PiB), ^{18}F-florbetaben (FBB), ^{18}F-florbetapir, ^{18}F-flutemetamol and ^{18}F-NAV4694 (NAV) are PET tracers that demonstrate binding to brain Aβ in AD from the preclinical AD stage onwards, with good sensitivity and specificity as biomarkers of antemortem AD pathology and predictors of progression to AD dementia [4-10]. Amyloid PET scans are used for inclusion and monitoring in AD-modifying clinical therapy trials, and to aid clinical diagnosis and prognostication [11].

Variability in tracers, PET scanners, procedural factors, and analysis methods across imaging centres have driven attempts for quantitative standardisation of amyloid PET results. Klunk and colleagues [12] derived a scale of 'Centiloid' units (CL) for standardised reporting of amyloid imaging. CL values range beyond the 'anchor-point' of 0, representing average young healthy controls, and 100, representing the amyloid burden present in average typical mild AD. This important work allows for amyloid PET scans across different sites to yield comparable results.

Comparison of neuropathological data with positive or negative amyloid PET scans based on expert visual read has been performed for ^{11}C-PiB, ^{18}F-florbetapir, ^{18}F-florbetaben and ^{18}F-flutemetamol [7, 9, 13-17]. In-vivo biomarkers such as cerebrospinal fluid Aβ, tau PET, and volumetric MRI have been compared with amyloid PET in CL [18, 19]. Only three recent studies, to our knowledge, have examined the performance of amyloid PET CL thresholds compared with SoT neuropathology [20-22].

We aim to define the accuracy of CL values when compared with SoT post-mortem neuropathological data on neuritic amyloid plaque density, final clinicopathological diagnosis of AD, and visual reading threshold for a positive amyloid PET scan.

Methods

Compliance with Ethical Standards

Ethics approval was obtained from the Austin Health Human Research Ethics Committee (reference LNR/17/405).

Subject identification and demographic data collection

Fifty-one subjects in total were retrospectively identified from the databases of the Austin Health Molecular Imaging and Therapy department, Sydney Brain and Mind Centre, and the Victorian Brain Bank. These subjects, with prior informed consent, had undergone both an amyloid PET scan and post-mortem neuropathologic brain evaluation between all years recorded in the database (2004 to 2017). Exclusion criteria for these prior studies were history of stroke, significant medical illness, recent cancer, and substance use disorder. Cases with a diagnosis of familial AD were excluded, as different neuropathological processes in this condition, such as a significantly greater density of Aβ plaques in the cerebellum than in sporadic AD [23, 24], may have confounded amyloid PET quantification and interpretation. Data has been published on a proportion of these cases [25, 26]. Two of the fifty-one subjects were excluded due to a diagnosis of familial AD.

Amyloid PET Imaging and Centiloid determination

Aβ imaging was performed with either ^{11}C-PiB or FBB. The methodology for PET imaging with these tracers has been previously described [27, 28]. A 20-minute acquisition was commenced 50 minutes post-injection of ^{11}C-PiB or 90 minutes post-injection of FBB. A transmission scan was performed for attenuation correction. PET images were reconstructed using a 3D row-action maximum likelihood algorithm (RAMLA). The standard Centiloid cortical and whole cerebellar volumes of interest template were applied to the summed and spatially normalized PET images in order to obtain standardized uptake value ratios (SUVR). For this study we used the CapAIBL software package, with a validated lower transformation to correct for CapAIBL registration without MRI [29, 30]. This package has been validated against the standard Centiloid MRI based spatial normalization with SPM8. The SUVR were transformed into Centiloid units by linear transformation using the PET tracer specific equations published for conversion of Centiloid method SUVR to Centiloid units with a minor correction applied for the CapAIBL registration [12, 27, 28, 31].

Neuropathologic evaluation

Neuropathological evaluation was performed at the Victorian Brain Bank (Melbourne, Australia) and Sydney Brain Bank (Neuroscience Research Australia, Sydney, Australia) to determine a global C score from inferior temporal regions of fixed brain hemispheres based on the Consortium for Establish a Registry for Alzheimer's Disease (CERAD) neuropathologic assessment guidelines [32]. Frequency of neuritic plaques per 100x microscopic field were categorised as none, sparse, moderate or frequent with corresponding C scores of 0, 1, 2 or 3 respectively, as described in published guidelines [33].

Visual Read

One amyloid PET expert reader (author CR), blinded to CL values and neuropathological data, visually interpreted all scans using MedView v12 software, viewing images in greyscale and rainbow colour scale. The method used to visually read amyloid PET has been previously described [34]. Scans were classified positive when cortical activity was equal to or greater than white matter activity in one or more lobes.

Clinicopathological diagnosis

The clinicopathological diagnosis for each case factored in both neuropathological assessment and antemortem clinical diagnosis. Neuropathological diagnosis was made in accordance with published guidelines [33], and included morphological examination with immunohistochemistry analyses for Aβ, tau, TDP43, and alpha-synuclein. There were 17 AD and 32 non-AD cases. Non AD cases included diagnoses of frontotemporal dementia (n=12), normal controls (n=3), dementia with Lewy bodies (n=3), Parkinson's disease dementia with concurrent diffuse Lewy bodies (n=3), hippocampal sclerosis (n=2), Creutzfeldt-Jakob disease (n=2), progressive supranuclear palsy (n=2), motor neuron disease (n=1), hippocampal ischaemia (n=1), corticobasal degeneration (n=1), multisystem atrophy (n=1), and a case of mixed AD and dementia with Lewy bodies (n =1) was excluded from being categorised as clinicopathological AD.

Statistical analyses

Three aspects of CL performance were investigated. Firstly, CL values were compared with dichotomized neuropathological C score categories using two different approaches: "high vs low" plaque density ("high" = moderate and frequent, and "low" = none and sparse), and; "any vs none" ("any" = sparse, moderate and frequent, and "none" = none). A Youden Index [35] was used to determine the optimal CL thresholds from receiver operator characteristic curves. Secondly, CL values were compared with binary

visual read (positive or negative). Thirdly, CL values were compared with cases of AD as determined by clinicopathological diagnosis using descriptive statistics. To assess for the any contribution of interval from PET scan to time to death, analyses were repeated using adjusted CL values, after applying a sigmoidal adjustment with a linear-segment accumulation rate of 5.18% per year, based on previous work by Villemagne and colleagues [36]. It should be noted that very low or very high degrees of amyloid neuropathology do not change as much as intermediate levels over time.

Results

Case Characteristics

Of the forty-nine included subjects, thirty-three underwent ^{11}C PiB PET and sixteen underwent FBB PET. Thirty-eight (78%) cases were male. The mean age at death was 76 years, and the median interval between date of last amyloid PET scan and death was 1005 (IQR ±1114) days.

Centiloid results and neuropathological C score categories

There were 19 (39%) patients with “high”, and 30 (61%) with “low” C scores. The receiver operator characteristic curve (Figure 1) demonstrated an area under curve (AUC) of 0.97 and an optimal threshold of 20.1 CL for detection of a high level of amyloid plaque (i.e. moderate or frequent neuritic plaques). After applying the sigmoidal adjustment for interval from scan to post-mortem, the putative optimal threshold was 21.3 CL.

Fig. 1 Centiloid results and “high” vs “low” C score categories

Receiver Operator Characteristic curve for Centiloid units thresholds in determining “high” vs “low” amyloid plaque burden

When neuritic plaque scores were grouped as to “any” (i.e. sparse or more) vs “none”, there were 24 (49%) with “any” and 25 (51%) with no neuritic plaques. The optimal CL threshold found for detecting the presence of any amyloid plaques (i.e. sparse or more) was 9.5 CL (Figure 2), with an AUC of 0.96, yielding a sensitivity of 0.96 and a specificity of 0.88. After applying the sigmoidal adjustment for interval from scan to post-mortem, the putative optimal threshold was 9.6 CL.

Fig. 2 Centiloid results and “none” vs “any” C score categories

Receiver Operator Characteristic curve for Centiloid units thresholds in determining “none” vs “any” amyloid plaque burden

Centiloid results and amyloid PET visual read

Correlation of Centiloid values with amyloid PET expert visual read (positive /negative) yielded an AUC of 1.0 and optimal CL threshold of 26. Using this threshold there was 100% agreement between Centiloid (elevated/not elevated) and visual read (positive/negative), (Figure 3).

Fig. 3 Centiloid results and amyloid PET visual read

Scatterplot for Centiloid unit threshold testing against binary expert visual read categories. A 26 CL cut-off yielded a 100% match to expert visual read of “high” or “low”.

Centiloid results in clinicopathological AD diagnosis

CL values were reviewed for the 17 cases that were determined to have a clinicopathological diagnosis of AD. The median CL result was 87.7 (IQR ±42.2), and 16 of the 17 cases (>90%) had a value of > 45 CL.

Discussion

Improving accuracy of the detection of brain amyloid plaques is important for clinical trial enrichment in the quest to develop disease-modifying or curative treatment for the growing burden of Alzheimer’s disease. Contemporary clinical application can also better assist diagnosis, prognostication and planning for patients with cognitive disorders.

We have demonstrated that a threshold of 20.1 CL was optimal for the detection of “high” levels of neuritic plaque density, as determined by C score moderate or frequent classification. In other words, values of 20.1 CL or lower accurately reflected the absence of moderate or frequent plaques, with a high AUC. This threshold was not significantly altered when corrected for time between scan and post-mortem. CL results below this threshold should provide reassurance that patients are unlikely to have Alzheimer’s disease. This is reasonably concordant with the findings of Navitsky and colleagues, who determined a threshold of 24.1 CL with florbetapir for CERAD amyloid plaque classification of moderate or frequent vs sparse or none, in 59 individuals [21]. This is also concordant with the Centiloid analysis by Dore and colleagues of a florbetaban phase III post-mortem study in 66 individuals, which yielded a threshold of 19 CL for the same categorisation [22]. These thresholds are higher than those identified by La Joie et al, who determined a threshold of 12.2 CL for separating none or sparse plaques from moderate or frequent plaques; and the same threshold of 12.2CL for separating any plaques from no plaques in 179

individuals scanned with ^{11}C-PiB PET [20]. Those authors did, however, acknowledge a contribution from false positive results, and suggested that 24 CL may be a more appropriate threshold for “identifying clinically meaningful Aβ burden,” and suggested the cut point of 19 CL proposed by Jack and colleagues [37] as a threshold predictive of reliable worsening of amyloid burden with time would be a more reasonable threshold to use. These thresholds may be useful as cut-offs for clinical trial enrichment, or for guiding decision-making about commencing potential disease-modifying therapies when they become available.

For the detection of “any” amyloid plaque (sparse or more), the optimal threshold identified was 9.5 CL. Once again, this value only marginally increased when corrected for time between scan and post-mortem. This threshold is similar to two standard deviations of young controls as determined by Klunk and colleagues, equalling 8.68 CL [12] and 12.2 CL [20]. This suggests there are no differences in amyloid tracer binding between young and old individuals with no amyloid plaques, indicating no substantial increase in non-specific binding nor significant changes in tracer kinetics with normal ageing.

A threshold of 26 CL exactly matched expert visual read of positive vs negative scan. This is consistent with good concordance (97%) noted by Leuzy and colleagues [18] between visual read and PiB CL results. Larger numbers of more borderline cases to better assess the correlation of CL result with visual read and identify the reasons for discordant classification may be warranted.

Our results compare favourably with phase III trials of PET tracers that have compared blinded expert visual reads of amyloid imaging with post-mortem data, where moderate to frequent neuritic plaques (a “high” classification in our study) were considered positive. Florbetaben visual reads were reported as having sensitivity of 97.9% and specificity of 88.9% [15]. Florbetapir visual reads yielded sensitivity of 92% and specificity of 100% within a 2-year window between imaging and autopsy [14]. Flutemetamol visual reads in one study correlated with both original and modified CERAD criteria, yielded respective sensitivities of 91.9% and 90.8%, and specificities of 87.0% and 90.0% [16].

In our cases with clinicopathological AD, a median CL value of 87.7 was found at post-mortem, but with significant variability as demonstrated by the IQR of ±42.2 CL. Only one of these cases, scoring 20.1 CL, returned a result under 45 CL, suggesting that a sensitivity cut-off for defining clinicopathological AD should be considerably higher than that for detecting “high” amyloid plaques alone. For comparison, an upper SUVR threshold of normal in a healthy control PiB PET group was calculated, using the upper 95% confidence interval, to be 1.41 by Nordberg et al [38], equating to 34 CL as converted by Leuzy et al [18]. The latter group demonstrated median PiB PET results of 47.5 CL for Mild Cognitive Impairment and 84.1 CL for AD in their group. These studies did not include post-mortem evaluation. Larger numbers in future studies would help confirm if a clinicopathological diagnosis of AD is indeed rare when under 45 CL.

The exclusion of mixed dementia only resulted in one case with AD neuropathology not being included in the analysis due to coexisting Lewy body disease; it is unclear what effect mixed dementia would have on the concordance of clinical diagnosis and CL values.

Limitations

A limitation of the study is the data distribution, in that only two subjects had results between 15 and 35 CL, consequently restricting the ability to tightly define thresholds. Specifically, these subjects had results of 20.1 and 30.9 CL.

Another limitation is the time elapsed between scan and death. This averaged approximately three years. We have accounted for this using established correction calculations. Of note, the only case of clinicopathological diagnosis of AD below 45 CL measured 20.1 CL, 6 years before death; this only increased to 21.3 CL after time-interval correction. Familial AD cases were excluded from this study due to potential presence of neuritic amyloid plaques in the cerebellum [23], and the lower affinity of PiB to “cotton wool” plaques found in some presenilin mutations [39]. These cerebellar plaques could interfere with the scaling to SUVR, and return misleading low CL results not applicable to typical sporadic AD [24]. Separate characterisation of CL performance in familial AD is warranted.

Conclusions

In our cohort, values <9.5 CL accurately reflected the absence of any neuritic plaques, and >20.1 CL indicated the presence of at least moderate plaque density. These neuropathology-based Centiloid thresholds may be used to exclude a diagnosis of AD and to define groups for early intervention and other disease specific trials.

List Of Abbreviations

^{11}C-PiB – ^{11}C-Pittsburgh Compound B

Aβ – amyloid-beta

AD – Alzheimer’s disease

AUC – Area Under Curve

CERAD – Consortium for Establish a Registry for Alzheimer’s Disease

CL – Centiloid

FBB – ^{18}F-florbetaben

IQR – Interquartile range

MRI – magnetic resonance imaging

NAV – ^{18}F-NAV4694 (NAV)

PET – Positron emission tomography

RAMLA – row-action maximum likelihood algorithm

ROC – Receiver Operator Characteristic

SoT – Standard of truth

SUVR - standardized uptake value ratio

TDP43 - TAR DNA-binding protein 43

Declarations

Ethical approval:

All procedures performed in studies involving human participants were in accordance with the Austin Health Human Research Ethics Committee (reference LNR/17/405) and with the 1964 Helsinki declaration and its later amendments or comparable ethical standards.

Consent for publication

All subjects had given consent for their data to be used for research purposes.

Availability of data

Data analysed in this study are available from the corresponding author on reasonable request.

Competing Interests and Funding:

Austin Health and Florey Institute of Neuroscience and Mental Health researchers are supported by governmental funding.

The Sydney Brain Bank is supported by the University of New South Wales and Neuroscience Research Australia.

The Victorian Brain Bank, supported by The Florey Institute of Neuroscience and Mental Health, The Alfred and the Victorian Forensic Institute of Medicine and funded in part by Parkinson's Victoria, MND Victoria, FightMND and Yulgilbar Foundation.

This imaging and prospective tissue donation for research from the Sydney cohort was supported by funding to ForeFront, a collaborative research group dedicated to the study of frontotemporal dementia and motor neurodegenerative diseases, from the National Health and Medical Research Council of

Australia (NHMRC) program (#1037746) and project (#630489) grants and the Australian Research Council Centre of Excellence in Cognition and its Disorders Memory Node (#CE110001021).

- Dr Amadoru is site principal investigator for the AbbVie ABBV-8E12 AWARE study at Austin Health. He receives a government hospital award wage for his Austin Health clinical and research appointments.
- Dr Doré reports no relevant disclosures.
- McLean reports no relevant disclosures.
- Ms Hinton reports no relevant disclosures.
- Dr Shepherd is the Director of the Sydney Brain Bank, which is funded by Neuroscience Research Australia and the University of New South Wales.
- Halliday is supported by a NHMRC Senior Principal Research Fellowship (#1079679).
- Dr Leyton is funded by an NHMRC dementia fellowship (APP1102969).
- Dr Yates is principal investigator on pharma-funded clinical trials including Novartis and Amgen and has received research funding from the Dementia Collaborative Research Centres (DCRC) and Eastern Melbourne Primary Healthcare Network (EMPHN).
- Hodges is supported by a NHMRC Senior Principal Research Fellowship (#1079679) and receives royalties from Oxford University Press related to book publication.
- Masters reports no relevant disclosures.
- Rowe reports no relevant disclosures.
- Prof Villemagne reports consultancies for Lundbeck, Hoffmann La Roche and Shanghai Green Valley Co., Ltd and speaking honoraria from Eli Lilly and Company, GE Healthcare and Fundació ACE (Barcelona), all outside the submitted work.

Author contributions

Name	Location	Role	Contribution
Sanka Amadoru, MBBS	Austin Health, Melbourne, Australia	Author	Study design, data acquisition and analysis; manuscript drafting and revision for intellectual content.
Vincent Dore, PhD	Austin Health and CSIRO, Melbourne, Australia	Author	Major role in data acquisition and analysis; revised the manuscript for intellectual content.
Catriona McLean, MD	Victorian Brain Bank, Melbourne Australia	Author	Major role in data acquisition and interpretation; revised the manuscript for intellectual content.
Fairlie Hinton	Victorian Brain Bank, Melbourne Australia	Author	Role in data acquisition; revised the manuscript for intellectual content.
Claire Shepherd, PhD	Sydney Brain Bank, Sydney, Australia	Author	Major role in data acquisition and interpretation; revised the manuscript for intellectual content.
Glenda Halliday, PhD	Sydney Brain Bank and University of Sydney, Sydney, Australia	Author	Major role in data acquisition and interpretation; revised the manuscript for intellectual content.
Cristian E. Leyton, PhD	University of Sydney, Sydney, Australia	Author	Role in data acquisition, data analysis and interpretation; revised the manuscript for intellectual content.
Paul Yates, PhD	Austin Health, Melbourne, Australia	Author	Role in data acquisition, data analysis and interpretation; revised the manuscript for intellectual content.
John Hodges, MD	University of Sydney, Sydney, Australia	Author	Minor role in data acquisition; revised the manuscript for intellectual content.
Colin L Masters, MD	Victorian Brain Bank, Melbourne Australia	Author	Minor role in data acquisition; revised the manuscript for intellectual content.
Victor L Villemagne, MD	Austin Health, Melbourne, Australia	Author	Major role in data acquisition, analysis and interpretation; revised the manuscript for intellectual content.
Christopher C Rowe, MD	Austin Health, Melbourne, Australia	Author	Major role in study design; data acquisition, analysis and interpretation; revised the manuscript for intellectual content.

Acknowledgments and author's information

Not applicable

References

1. Hyman BT, Phelps CH, Beach TG, Bigio EH, Cairns NJ, Carrillo MC, et al. National Institute on Aging-Alzheimer's Association guidelines for the neuropathologic assessment of Alzheimer's disease. Alzheimers Dement. 2012;8:1-13. doi:10.1016/j.jalz.2011.10.007.
2. Dubois B, Feldman HH, Jacova C, Hampel H, Molinuevo JL, Blennow K, et al. Advancing research diagnostic criteria for Alzheimer's disease: the IWG-2 criteria. Lancet Neurol. 2014;13:614-29. doi:10.1016/S1474-4422(14)70090-0.
3. Jack CR, Jr., Bennett DA, Blennow K, Carrillo MC, Dunn B, Haeberlein SB, et al. NIA-AA Research Framework: Toward a biological definition of Alzheimer's disease. Alzheimers Dement. 2018;14:535-62. doi:10.1016/j.jalz.2018.02.018.
4. Wiley CA, Lopresti BJ, Venneti S, Price J, Klunk WE, DeKosky ST, et al. Carbon 11-labeled Pittsburgh Compound B and carbon 11-labeled (R)-PK11195 positron emission tomographic imaging in Alzheimer disease. Arch Neurol. 2009;66:60-7. doi:10.1001/archneurol.2008.511.
5. Sperling RA, Johnson KA, Doraiswamy PM, Reiman EM, Fleisher AS, Sabbagh MN, et al. Amyloid deposition detected with florbetapir F 18 ((18)F-AV-45) is related to lower episodic memory performance in clinically normal older individuals. Neurobiol Aging. 2013;34:822-31. doi:10.1016/j.neurobiolaging.2012.06.014.
6. Doraiswamy PM, Sperling RA, Johnson K, Reiman EM, Wong TZ, Sabbagh MN, et al. Florbetapir F 18 amyloid PET and 36-month cognitive decline: a prospective multicenter study. Mol Psychiatry. 2014;19:1044-51. doi:10.1038/mp.2014.9.
7. Beckett TL, Webb RL, Niedowicz DM, Holler CJ, Matveev S, Baig I, et al. Postmortem Pittsburgh Compound B (PiB) binding increases with Alzheimer's disease progression. J Alzheimers Dis. 2012;32:127-38. doi:10.3233/JAD-2012-120655.
8. Sabri O, Seibyl J, Rowe C, Barthel H. Beta-amyloid imaging with florbetaben. Clin Transl Imaging. 2015;3:13-26. doi:10.1007/s40336-015-0102-6.
9. Thurfjell L, Lilja J, Lundqvist R, Buckley C, Smith A, Vandenberghe R, et al. Automated quantification of 18F-flutemetamol PET activity for categorizing scans as negative or positive for brain amyloid: concordance with visual image reads. J Nucl Med. 2014;55:1623-8. doi:10.2967/jnumed.114.142109.
10. Rowe CC, Pejoska S, Mulligan RS, Jones G, Chan JG, Svensson S, et al. Head-to-head comparison of 11C-PiB and 18F-AZD4694 (NAV4694) for beta-amyloid imaging in aging and dementia. J Nucl Med. 2013;54:880-6. doi:10.2967/jnumed.112.114785.
11. Schonecker S, Prix C, Raiser T, Ackl N, Wlasich E, Stenglein-Krapf G, et al. [Amyloid positron-emission-tomography with [18 F]-florbetaben in the diagnostic workup of dementia patients]. Nervenarzt. 2017;88:156-61. doi:10.1007/s00115-016-0249-z.
12. Klunk WE, Koeppe RA, Price JC, Benzinger TL, Devous MD, Sr., Jagust WJ, et al. The Centiloid Project: standardizing quantitative amyloid plaque estimation by PET. Alzheimers Dement. 2015;11:1-15 e1-4. doi:10.1016/j.jalz.2014.07.003.

13. Choi SR, Schneider JA, Bennett DA, Beach TG, Bedell BJ, Zehntner SP, et al. Correlation of amyloid PET ligand florbetapir F 18 binding with Abeta aggregation and neuritic plaque deposition in postmortem brain tissue. Alzheimer Dis Assoc Disord. 2012;26:8-16. doi:10.1097/WAD.0b013e31821300bc.
14. Clark CM, Pontecorvo MJ, Beach TG, Bedell BJ, Coleman RE, Doraiswamy PM, et al. Cerebral PET with florbetapir compared with neuropathology at autopsy for detection of neuritic amyloid-beta plaques: a prospective cohort study. Lancet Neurol. 2012;11:669-78. doi:10.1016/S1474-4422(12)70142-4.
15. Sabri O, Sabbagh MN, Seibyl J, Barthel H, Akatsu H, Ouchi Y, et al. Florbetaben PET imaging to detect amyloid beta plaques in Alzheimer's disease: phase 3 study. Alzheimers Dement. 2015;11:964-74. doi:10.1016/j.jalz.2015.02.004.
16. Salloway S, Gamez JE, Singh U, Sadowsky CH, Villena T, Sabbagh MN, et al. Performance of [(18)F]flutemetamol amyloid imaging against the neuritic plaque component of CERAD and the current (2012) NIA-AA recommendations for the neuropathologic diagnosis of Alzheimer's disease. Alzheimers Dement (Amst). 2017;9:25-34. doi:10.1016/j.dadm.2017.06.001.
17. Curtis C, Gamez JE, Singh U, Sadowsky CH, Villena T, Sabbagh MN, et al. Phase 3 trial of flutemetamol labeled with radioactive fluorine 18 imaging and neuritic plaque density. JAMA Neurol. 2015;72:287-94. doi:10.1001/jamaneurol.2014.4144.
18. Leuzy A, Chiotis K, Hasselbalch SG, Rinne JO, de Mendonca A, Otto M, et al. Pittsburgh compound B imaging and cerebrospinal fluid amyloid-beta in a multicentre European memory clinic study. Brain. 2016;139:2540-53. doi:10.1093/brain/aww160.
19. Jack CR, Jr., Wiste HJ, Weigand SD, Therneau TM, Knopman DS, Lowe V, et al. Age-specific and sex-specific prevalence of cerebral beta-amyloidosis, tauopathy, and neurodegeneration in cognitively unimpaired individuals aged 50-95 years: a cross-sectional study. Lancet Neurol. 2017;16:435-44. doi:10.1016/S1474-4422(17)30077-7.
20. La Joie R, Ayakta N, Seeley WW, Borys E, Boxer AL, DeCarli C, et al. Multisite study of the relationships between antemortem [(11)C]PIB-PET Centiloid values and postmortem measures of Alzheimer's disease neuropathology. Alzheimers Dement. 2018. doi:10.1016/j.jalz.2018.09.001.
21. Navitsky M, Joshi AD, Kennedy I, Klunk WE, Rowe CC, Wong DF, et al. Standardization of amyloid quantitation with florbetapir standardized uptake value ratios to the Centiloid scale. Alzheimers Dement. 2018. doi:10.1016/j.jalz.2018.06.1353.
22. Dore V SB, Rowe CC, Bourgeat P, Sabri O, Stephens A, Barthel H, Fripp J, Masters CL, Dinkelborg L, Salvado O, Villemagne VL, Desanti S. . Comparison of 18F-florbetaben quantification results using the standard Centiloid, MR-based and MR-Less CapAIBL® approaches: Validation against histopathology. . Alz and Dementia. In press, accepted 12/3/2019.
23. Mann DM, Pickering-Brown SM, Takeuchi A, Iwatsubo T, Members of the Familial Alzheimer's Disease Pathology Study G. Amyloid angiopathy and variability in amyloid beta deposition is

determined by mutation position in presenilin-1-linked Alzheimer's disease. Am J Pathol. 2001;158:2165-75.

24. Klunk WE, Price JC, Mathis CA, Tsopelas ND, Lopresti BJ, Ziolko SK, et al. Amyloid deposition begins in the striatum of presenilin-1 mutation carriers from two unrelated pedigrees. J Neurosci. 2007;27:6174-84. doi:10.1523/JNEUROSCI.0730-07.2007.
25. Tan RH, Kril JJ, Yang Y, Tom N, Hodges JR, Villemagne VL, et al. Assessment of amyloid beta in pathologically confirmed frontotemporal dementia syndromes. Alzheimers Dement (Amst). 2017;9:10-20. doi:10.1016/j.dadm.2017.05.005.
26. Leyton CE, Villemagne VL, Savage S, Pike KE, Ballard KJ, Piguet O, et al. Subtypes of progressive aphasia: application of the International Consensus Criteria and validation using beta-amyloid imaging. Brain. 2011;134:3030-43. doi:10.1093/brain/awr216.
27. Rowe CC, Dore V, Jones G, Baxendale D, Mulligan RS, Bullich S, et al. 18F-Florbetaben PET beta-amyloid binding expressed in Centiloids. Eur J Nucl Med Mol Imaging. 2017;44:2053-9. doi:10.1007/s00259-017-3749-6.
28. Rowe CC, Jones G, Dore V, Pejoska S, Margison L, Mulligan RS, et al. Standardized Expression of 18F-NAV4694 and 11C-PiB beta-Amyloid PET Results with the Centiloid Scale. J Nucl Med. 2016;57:1233-7. doi:10.2967/jnumed.115.171595.
29. Bourgeat P, Villemagne VL, Dore V, Brown B, Macaulay SL, Martins R, et al. Comparison of MR-less PiB SUVR quantification methods. Neurobiol Aging. 2015;36 Suppl 1:S159-66. doi:10.1016/j.neurobiolaging.2014.04.033.
30. Zhou L, Salvado O, Dore V, Bourgeat P, Raniga P, Macaulay SL, et al. MR-less surface-based amyloid assessment based on 11C PiB PET. PLoS One. 2014;9:e84777. doi:10.1371/journal.pone.0084777.
31. Bourgeat P, Dore V, Fripp J, Ames D, Masters CL, Salvado O, et al. Implementing the centiloid transformation for (11)C-PiB and beta-amyloid (18)F-PET tracers using CapAIBL. Neuroimage. 2018;183:387-93. doi:10.1016/j.neuroimage.2018.08.044.
32. Mirra SS, Heyman A, McKeel D, Sumi SM, Crain BJ, Brownlee LM, et al. The Consortium to Establish a Registry for Alzheimer's Disease (CERAD). Part II. Standardization of the neuropathologic assessment of Alzheimer's disease. Neurology. 1991;41:479-86.
33. Montine TJ, Phelps CH, Beach TG, Bigio EH, Cairns NJ, Dickson DW, et al. National Institute on Aging-Alzheimer's Association guidelines for the neuropathologic assessment of Alzheimer's disease: a practical approach. Acta Neuropathol. 2012;123:1-11. doi:10.1007/s00401-011-0910-3.
34. Rowe CC, Villemagne VL. Brain amyloid imaging. J Nucl Med Technol. 2013;41:11-8. doi:10.2967/jnumed.110.076315.
35. Ruopp MD, Perkins NJ, Whitcomb BW, Schisterman EF. Youden Index and optimal cut-point estimated from observations affected by a lower limit of detection. Biom J. 2008;50:419-30. doi:10.1002/bimj.200710415.
36. Villemagne VL, Burnham S, Bourgeat P, Brown B, Ellis KA, Salvado O, et al. Amyloid beta deposition, neurodegeneration, and cognitive decline in sporadic Alzheimer's disease: a prospective cohort study.

Lancet Neurol. 2013;12:357-67. doi:10.1016/S1474-4422(13)70044-9.

37. Jack CR, Jr., Wiste HJ, Weigand SD, Therneau TM, Lowe VJ, Knopman DS, et al. Defining imaging biomarker cut points for brain aging and Alzheimer's disease. Alzheimers Dement. 2017;13:205-16. doi:10.1016/j.jalz.2016.08.005.
38. Nordberg A, Carter SF, Rinne J, Drzezga A, Brooks DJ, Vandenberghe R, et al. A European multicentre PET study of fibrillar amyloid in Alzheimer's disease. Eur J Nucl Med Mol Imaging. 2013;40:104-14. doi:10.1007/s00259-012-2237-2.
39. Ikonomovic M AE, Price J, Mathis M, Klunk W. Evaluation of cotton wool plaques using amyloid binding compounds and Aβ immunohistochemistry: implications for PiB PET imaging. (abst). Human Amyloid Imaging Handbook; 2014. p. 41.

Figures

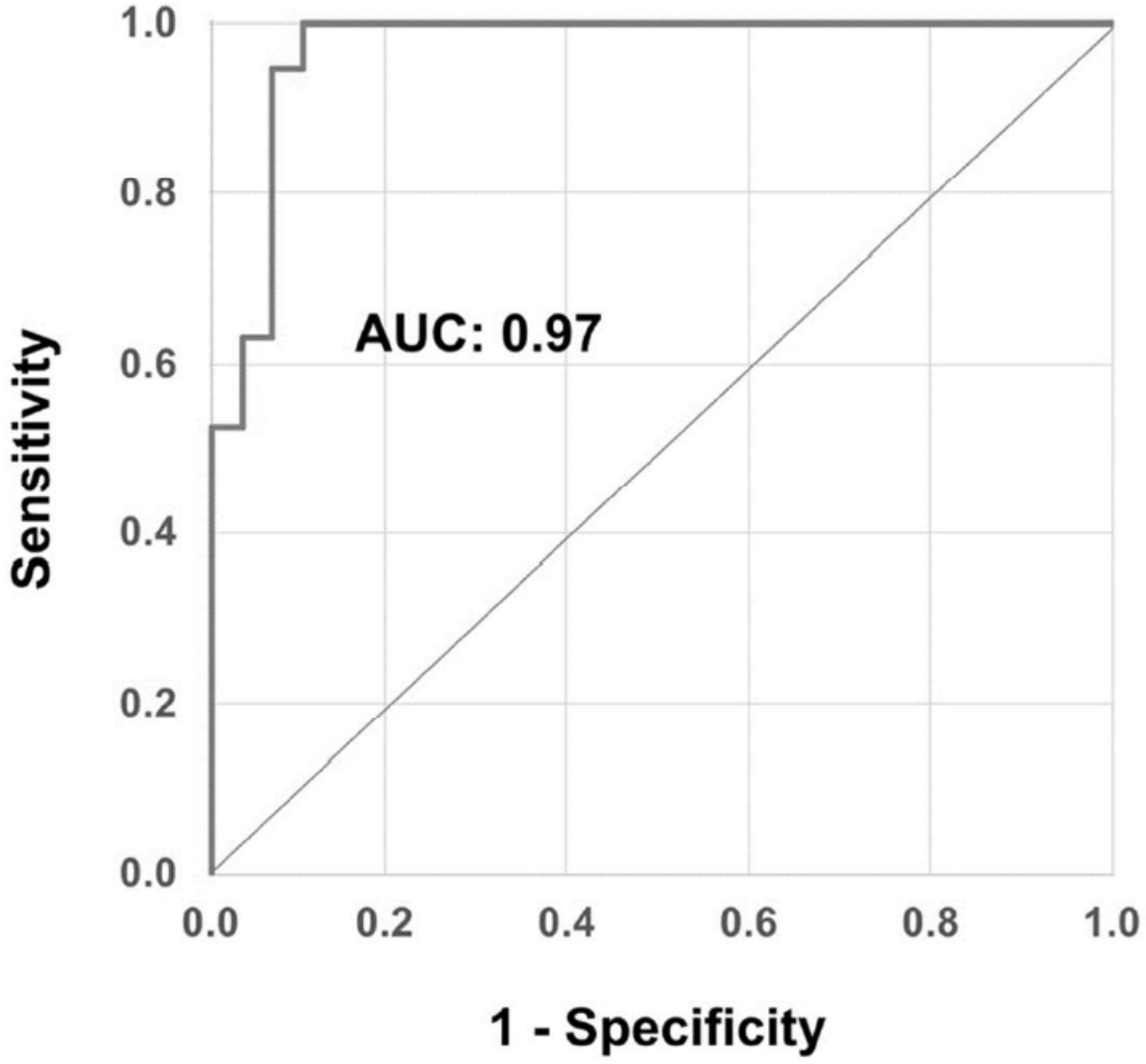

Figure 1

Centiloid results and “high” vs “low” C score categories Receiver Operator Characteristic curve for Centiloid units thresholds in determining “high” vs “low” amyloid plaque burden

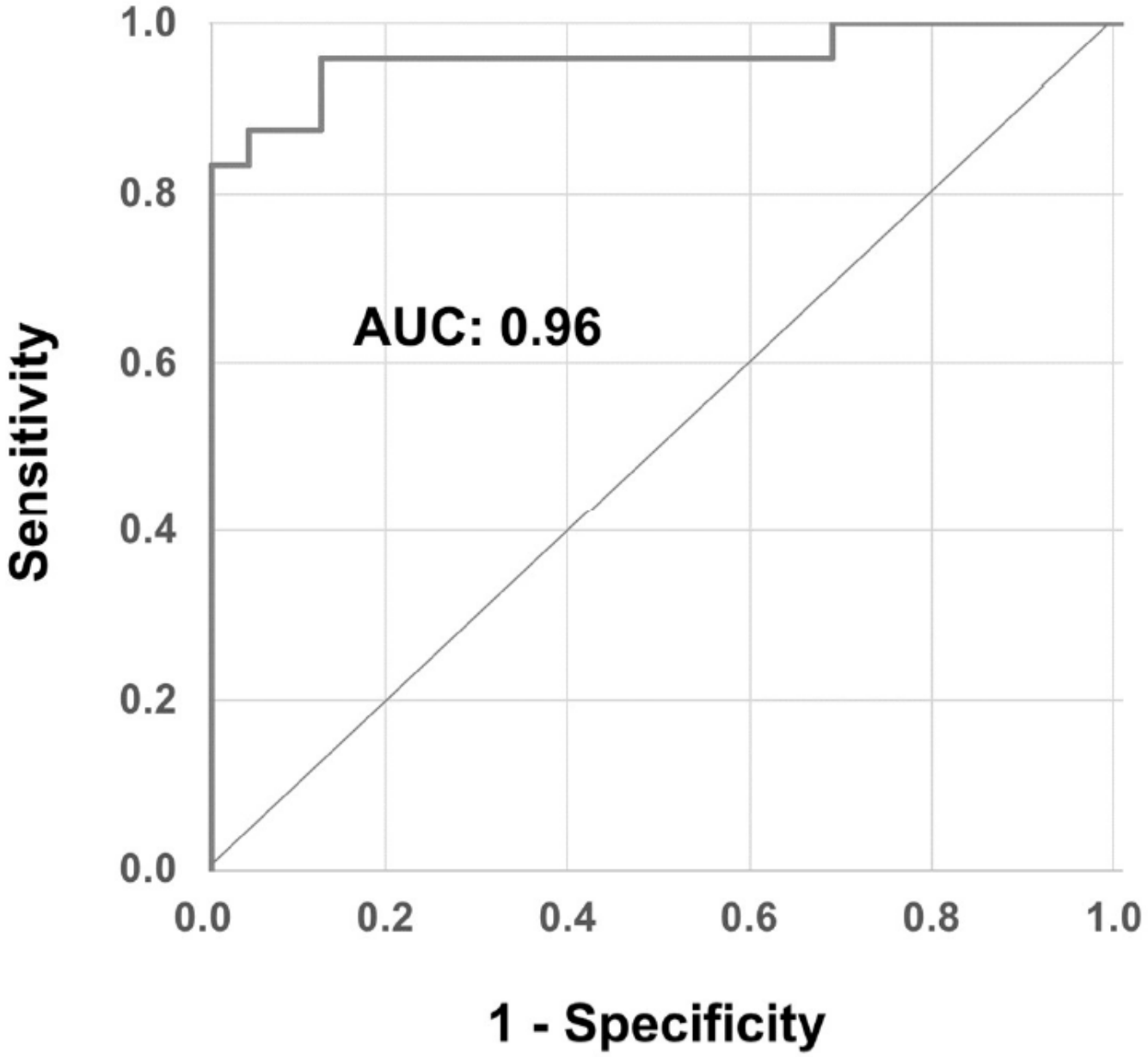

Figure 2

Centiloid results and “none” vs “any” C score categories Receiver Operator Characteristic curve for Centiloid units thresholds in determining “none” vs “any” amyloid plaque burden

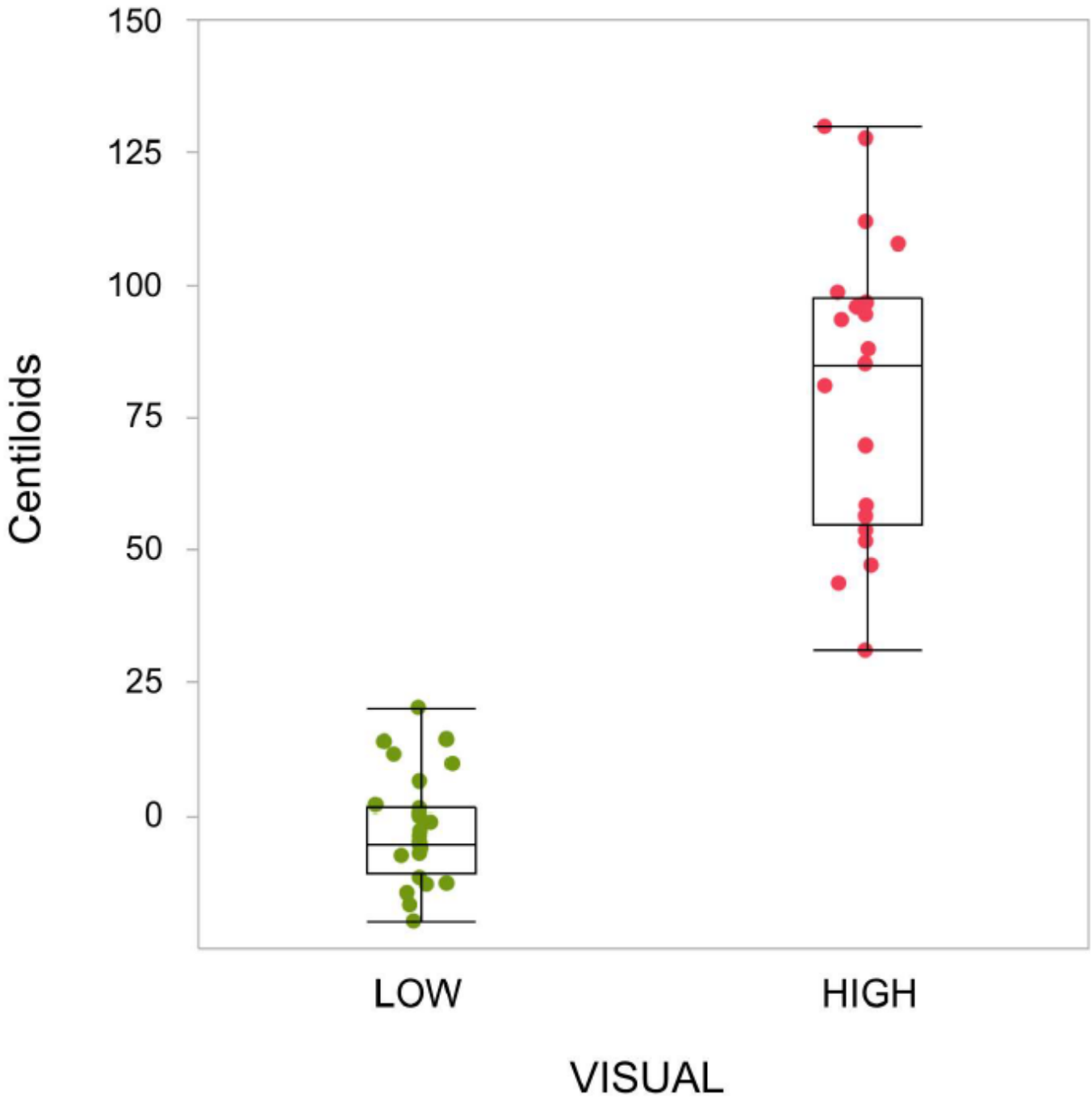

Figure 3

Centiloid results and amyloid PET visual read Scatterplot for Centiloid unit threshold testing against binary expert visual read categories. A 26 CL cut-off yielded a 100% match to expert visual read of “high” or “low”.